



Towards Self-shaping Metamaterial Shells: A Computational Design Workflow for Hybrid Additive Manufacturing of Architectural Scale Double-Curved Structures

E. Özdemir^(✉), L. Kiesewetter^(✉), K. Antorveza^(✉), T. Cheng, S. Leder, D. Wood,
and A. Menges

Institute for Computational Design and Construction, Keplerstr. 11, 70174 Stuttgart, Germany
{icd.mail,e.ozdemir,laura.kiesewetter,icd.mail,
k.antorveza}@icd.uni-stuttgart.de

Abstract. Double curvature enables elegant and material-efficient shell structures, but their construction typically relies on heavy machining, manual labor, and the additional use of material wasted as one-off formwork. Using a material's intrinsic properties for self-shaping is an energy and resource-efficient solution to this problem. This research presents a fabrication approach for self-shaping double-curved shell structures combining the hygroscopic shape-changing and scalability of wood actuators with the tunability of 3D-printed metamaterial patterning. Using hybrid robotic fabrication, components are additively manufactured flat and self-shape to a pre-programmed configuration through drying. A computational design workflow including a lattice and shell-based finite element model was developed for the design of the metamaterial pattern, actuator layout, and shape prediction. The workflow was tested through physical prototypes at centimeter and meter scales. The results show an architectural scale proof of concept for self-shaping double-curved shell structures as a resource-efficient physical form generation method.

Keywords: Self-shaping wood · 3D printing · Robotic fabrication · Mechanical metamaterials · Material programming

1 Introduction

Shell structures are advantageous in architecture because the geometric stiffness resulting from the double curvature makes them highly material-efficient [1]. Recent advancement in computational modeling and simulation technology gives architects and engineers sophisticated tools to design elegant and geometrically performative structures with ease [2, 3]. However, constructing double-curved designs with conventional construction techniques is laborious and requires complicated machining or large formwork with excessive waste production. On the construction site, forming or using large formwork depend highly on skilled manual labor and intricate scaffolding [4].

This research proposes an alternative to contemporary shell construction practice: By using a material's intrinsic properties, forming instructions can be embedded into the

material system and conventional forming methods can be replaced with self-shaping. The structure is made of a hybrid material system combining self-shaping wood actuators with a tunable 3D-printed metamaterial patterning (MMP). It is designed to be fabricated in a flat configuration, reducing the complications and excess of 3D forming. It then autonomously self-shapes on-site into the pre-programmed double-curved geometry (Fig. 1). The shape can then be locked by constraining the edges or inter parts of the structure to avoid further deformation.

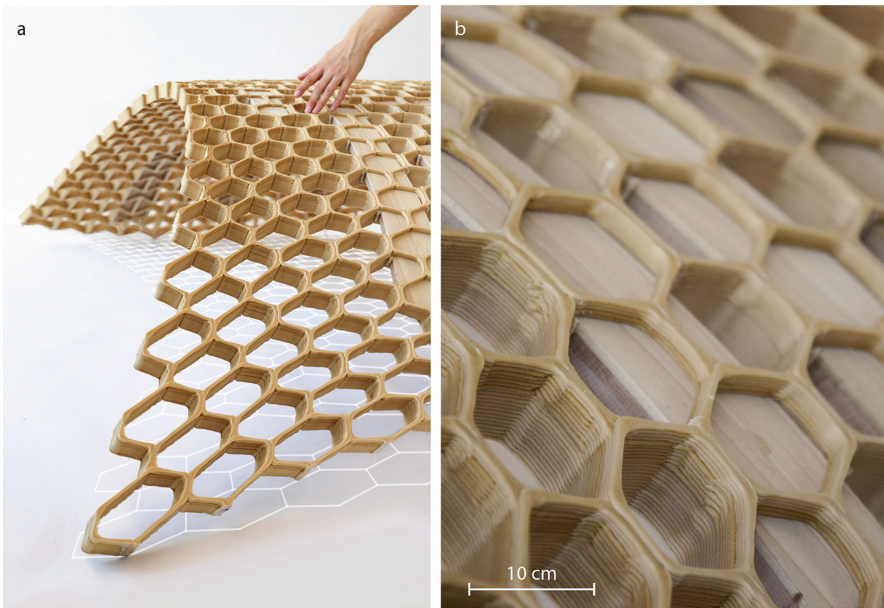


Fig. 1. (a) A lightweight, self-shaped double-curved shell structure manufactured additively from 3D-printed bio-composite metamaterial patterning (MMP) and integrated wood actuators. (b) Detail of the stiffness-tunable patterning and actuator connection

1.1 Self-shaping Structures

The development of self-shaping systems is a growing field of research in material science and engineering. Geometric self-shaping mechanisms in planar lattices have been demonstrated on smaller scales [5, 6]. At a similar scale, prestressed reinforced elastic membranes have been used for deployable elements that spring from flat to curved when released [7]. These systems are scalable but require control of high stresses at deployment.

Self-shaping Wood. In the form of a bilayer, wood becomes a natural actuator that generates curvature. It is both hygroscopic and anisotropic, which makes it respond to its surrounding relative humidity (RH) with shape changes depending on its grain direction and wood moisture content (WMC) [8, 9]. When used for shaping large curved timber elements, wood bilayers are fabricated flat and self-shape during drying [10].

Although single curvature can be achieved from wood bilayers, the creation of double curvature in solid wood plates is only achievable to a limited extent and difficult to predict [11]. Self-shaping wood gridshells have also been investigated with finite element (FE) models and tabletop prototypes but have limited design freedom so far [12]. The principle of self-shaping wood actuators combined with a 3D-printed structure for single-curved geometries has been studied with prototypes on a similar scale [13].

1.2 Large Scale Additive Manufacturing (LSAM)

Large Scale Additive Manufacturing (LSAM) is a high-resolution additive fabrication method that enables tuning on a local level. Lightweight, filigree structures can be designed and printed with specific local bending properties and bent into shape. These properties allow for the creation of shell structures with little to no waste production but still require extensive and coordinated physical shaping on-site [14].

1.3 Bending-Active Metamaterial Surfaces

Auxetics are a class of metamaterials that show unusual behavior when stretched or compressed due to their engineered geometry that causes negative Poisson's ratio [15]. Unlike most other bending-active plate materials that create single curvature when bent [16], these materials can create double curvature [17]. By carefully designing these MMPs, the resulting bent geometry can be pre-programmed to exhibit anticlastic, single curved, and synclastic areas [18]. The potentials of this principle for building structures have so far only been explored on a small scale due to the significant forces required to bend larger structures.

2 Methods

Our approach focuses on the computational design and fabrication of a 3D-printed auxetic MMP with integrated wood bilayer actuators to achieve self-shaping shell structures at a large scale. The concept is investigated through the development of a computational design workflow (Fig. 2), validated with a 1:10 scale physical prototype, and a full-scale demonstrator.

2.1 Design and Analysis

The computational design workflow starts with the design of a double-curved shell geometry in which surface curvature is adjusted within a range related to the bending stiffness of the materials. The design intent is evaluated through curvature and structural analysis: While the structural analysis is used to determine where to reinforce the geometry with increased stiffness through a gradient in structural depth, the curvature analysis plays a key role in designing the MMP and determining the actuator locations and orientations.

Since predicting the behavior of a hybrid material system is complex, physical tests are used to understand the relationship between the wood actuators and the 3D-printed MMP.

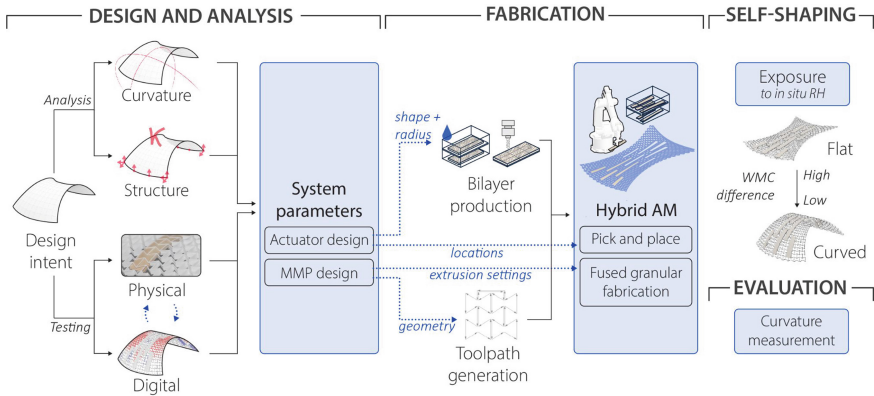


Fig. 2. Computational design workflow overview: defining the system parameters, hybrid additive manufacturing (AM) of the prototypes, self-shaping through drying and evaluation

A simulation is also developed as a design tool allowing for quick design iterations with the feedback of both structural and shaping parameters. In parallel, scaled physical prototypes (1:10) are produced to test the simulation accuracy and to validate the self-shaping of the structure. The scaled physical prototypes are geometrically compared to the outcome of the simulation, and the self-shaping parameters are calibrated until satisfactory results are achieved. Based on a chosen configuration, the wood actuators are produced and the fabrication instructions for the LSAM are generated.

2.2 Physical and Digital Testing

While physical tests (Fig. 3) are essential to study the complex relations between different design parameters, they are time and material-consuming. The simulation tool developed for this research combines Timoshenko's bimetal theory [19] and a lattice-based model with varying expansion coefficients [20, 21] using an incremental solver for large deformation analyses in Karamba 3D [22]. Restrictive and active layers of the actuators are represented by a lattice of beams, rigidly connected in each node. The external stimulus for shrinkage in the active layer is represented by changes in the thermal load with the corresponding thermal expansion coefficient. The radius achieved by the bilayers in the simulation is compared and calibrated to actuated physical wood bilayers. The 3D-printed pattern is modeled as a system of vertically oriented shell elements with mechanical properties matching that of the printed material, rigidly connected to the lattice structure of the bilayers.

2.3 Hybrid Additive Manufacturing

First, the wood actuators are produced from passive layers and active layers that were equalized at 92% (RH) for a month. Subsequently, they are CNC milled into their final shapes and once again put back into the moisture chamber until the start of the hybrid additive manufacturing process.

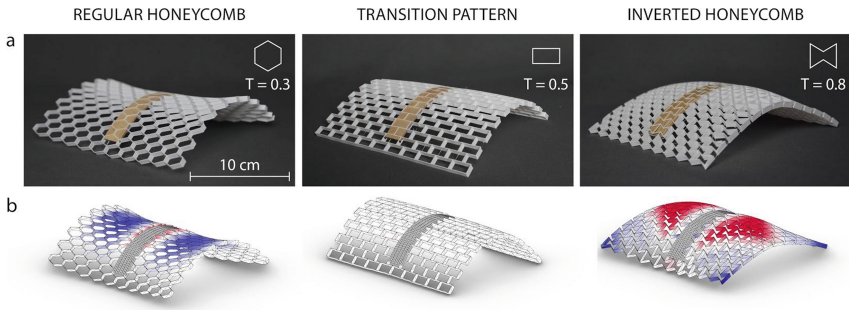


Fig. 3. Initial cm scale tests showing variable MMPs' influence on curvature. (a) Physical tests with variations in cell geometry to produce anticlastic, single curved, and synclastic bending with a desktop fused deposition modeling (FDM) printer, polylactide (PLA) filament, and a wood veneer bilayer actuator. (b) Initial digital tests with variations in cell geometry (T = angular parameter determining concavity)

To 3D-print the MMP, a single continuous polyline is created for the G-Code generation [23]. The base layers are the first to be 3D-printed using robotic LSAM, leaving pockets for the actuators. Then, the actuators are inserted into the MMP, and enclosure layers are printed on top.

2.4 On-site Self-shaping

Once the fabrication is completed, the structure is wrapped in airtight packaging and flat-transported to the deployment site. There, it is allowed to dry in ambient humidity conditions, gradually decreasing the WMC and self-shaping into the final structure.

3 Prototyping and Results

Before upscaling the system, the developed workflow was tested using a small-scale physical prototype (1:10) to ensure that the design parameters could meet the geometrical and behavioral expectations. After this preliminary study, the design was scaled up ten times and a full-scale demonstrator was produced to prove the scalability of the material system.

3.1 Small Scale Prototype

A shell geometry was designed to self-erect from the ground as much as possible from a 60 cm \times 20 cm flat pattern while exhibiting areas of anticlastic, single, and synclastic curvature (Fig. 4). The pattern was printed in three pieces and embedded with eleven actuators made from 3 mm thick beech-maple bilayers. The three pieces were assembled by using glue and were left in interior ambient conditions (40% RH) to self-shape as a single structure in 36 h (Fig. 4c). The resulting self-shaping geometry achieved reasonable approximations to the simulation prediction, although continuous curvature was not achieved most likely due to the gradient being interrupted between the pieces.

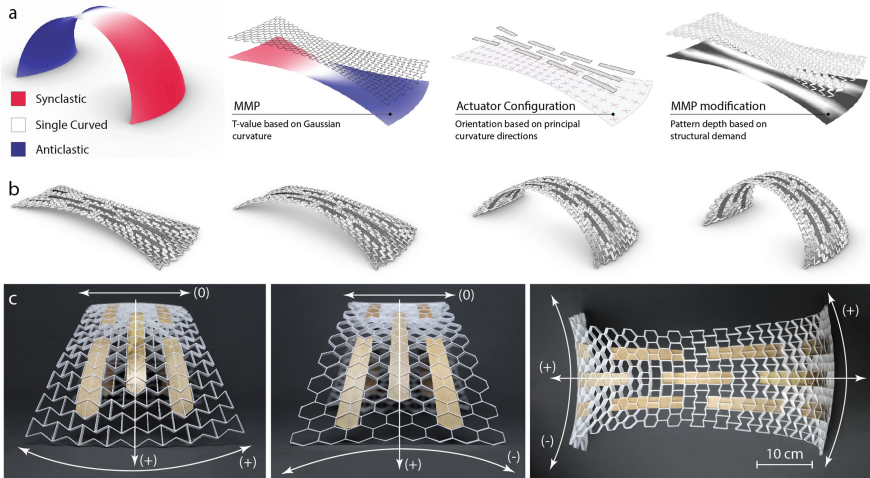


Fig. 4. Small scale prototype. (a) Gaussian curvature values of the goal geometry are used to adjust the MMP, actuators are placed on the cells with the highest first principal curvature. Depth gradient is applied to ensure curvature continuity. (b) FE simulation of self-shaping structure. (c) Results of self-shaping in 1:10 physical prototype

3.2 Large Scale Demonstrator

The significant shift in the scale and self-weight required recalibration of the parameters in the computational design workflow. The cell sizes and actuator placement were adapted for the workspace ($3.0 \text{ m} \times 1.5 \text{ m}$ table) of a robotic LSAM setup incorporating a 6-axis industrial robot (Kuka KRC420) equipped with a Fused Granular Fabrication extrusion system (CEAD GB.V.). To achieve a stable geometry, local utilization values from the structural analysis were used to inform the depth gradient that reinforces the structure. The simulation was also adjusted to the increased cell size and pattern depth, as well as the new nozzle diameter (3 mm) and printing material, a cellulose-filled plastic bio-composite (UPM Formi 3D 20/19 - UPM). Two 3D-printed MMP specimens were subjected to a deflection test and compared to the simulation for calibration. The same approach was used to calibrate the model to the wood bilayers. A 16 mm thick bilayer, consisting of 12 mm beech conditioned to a WMC of $>25\%$ and 4 mm white wood was considered most suitable. For calibration, a sample actuator was left to dry unbound in indoor ambient conditions (ca. $25 \text{ }^\circ\text{C}/50\% \text{ RH}$). The final actuator placement was based on the comparison of simulation outcomes with the design intent.

The demonstrator was robotically fabricated in four sequential steps (Fig. 5a) within which the actuators were placed and encased during 15 consecutive hours.

The demonstrator with the overall dimensions of $250 \text{ cm} \times 150 \text{ cm}$ was produced in one piece using eleven embedded actuators (Fig. 5). The completed demonstrator was then left to self-shape in indoor conditions (ca. $21 \text{ }^\circ\text{C}/\text{RH } 35\%–47\%$). After 72 h, only minimal shape change was achieved due to the large self-weight of the prototype. To aid in the shaping process it was then supported from its center of gravity. In the next 80 h, the hanging demonstrator bent to the intended geometry and remained in the

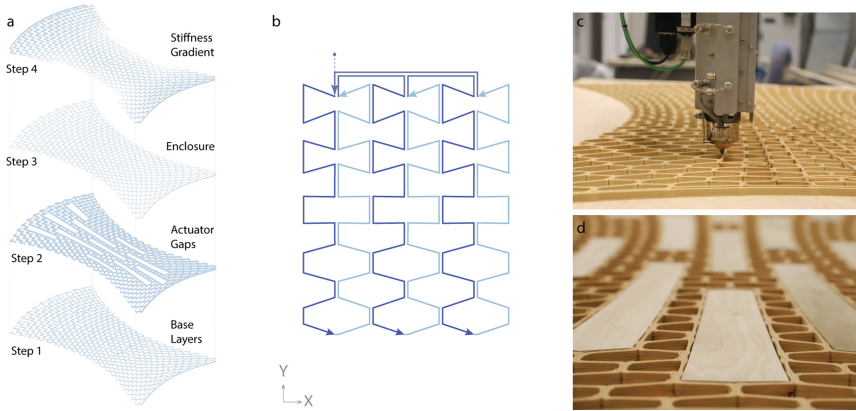


Fig. 5. Demonstrator fabrication. (a) MMP structure and sequential printing steps. (b) Detail of variations in the MMP and associated printing tool paths. (c) LSAM of the base layers. (d) Integration of the wood actuators within the tuned MMP before printing the enclosure layer

shaped configuration under its self-weight (Fig. 6a). Structural supports were added at the ends of the structure post shaping to prevent any further movement in the structure due to ambient condition changes. The shape retention was verified by 3D scanning the demonstrator (Fig. 6d) after over four months in ambient conditions and comparing the point cloud to the simulation.

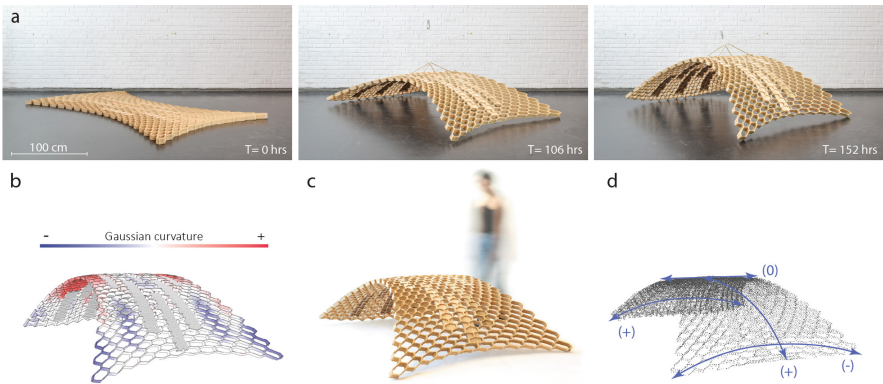


Fig. 6. Demonstrator. (a) Self-shaping sequence of the large-scale demonstrator over 152 h. (b) Predicted geometry from the simulation. (c) Self-shaped structure in the actuated state. (d) 3D laser scan of the self-shaped geometry with areas of synclastic (+/+), anticlastic (+/-) and single curved (0) bending

4 Discussion

The large-scale demonstrator showcases the potential of scaling up self-shaping wood and 3D-printed MMP to achieve double-curved shell geometries. We developed a

computational design workflow for pre-programming self-shaping surfaces with goal-geometry-oriented auxetic pattern generation and actuator orientation, resulting in a structure with embedded self-shaping information. Our simulation proved to be capable of predicting both the self-shaping process (Fig. 4) and the final geometry (Fig. 6b, d), serving as a useful design tool. Finally, we implemented an optimized printing sequence for the auxetic metamaterials, used during the robotic LSAM process. While the pre-programming of geometry with the developed workflow and upscaling of this material system were successful, the self-shaping process did not occur entirely as intended. The most notable issue resulted from the separation of the actuators and the MMP which caused stress-related failures and deviations from the model. This could have been avoided if the prototype was supported from the start of actuation, and by better integration of the actuators.

To improve the accuracy of the model, future research could incorporate moisture dependency of the mechanical properties of wood. The presented model was developed by relying on the inherent structural benefit of double-curved surfaces, therefore further work is needed to verify that the self-shaping is compatible with structural design requirements. Form stability after actuation is a known requirement of self-shaping processes applied in construction. The addition of supports at the edges of the structure or the usage of tension cables to lock areas of the geometry as used in gridshell structures could increase the structural stability after self-shaping. Another interesting approach is to lock the geometry using integrated snap-fit locking mechanisms (Fig. 7) that could be included in the printing of the MMP.

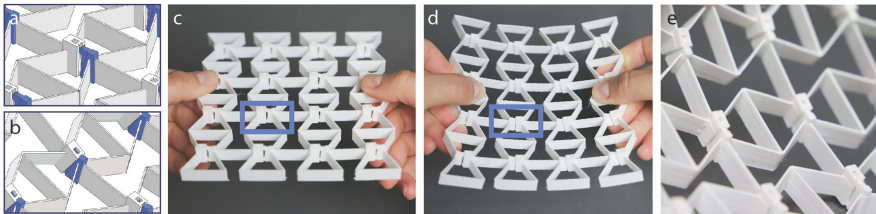


Fig. 7. Initial development of an integrated 3D-printed snap-fit locking mechanism. (a) Flat state diagram. (b) Bent state diagram. (c) Physical prototype flexible state. (d) Physical prototype locked state. (e) Locking mechanism detail

5 Conclusion

A computational design workflow was developed for designing and predicting self-shaping hybrid structures. The framework was tested through two physical prototypes at different scales, demonstrating how MMP can be used for self-shaping architectural scale double-curved structures. This system can be adopted for the construction of shells that are typically structurally well-performing, but which are usually avoided due to the difficult production and erection processes. We envision a construction approach that achieves complex 3D geometries from simplified 2.5D fabrication, with the potential of

reducing carbon footprint through flat-packed transportation and decreasing labor and scaffolding by self-shaping on-site (Fig. 8). With further improvements to the fabrication setup, the research presented offers a low-impact solution for the construction of complex architectural structures. In this way, it contributes environmentally and technologically to the way we build, taking a step towards more sustainable construction methods.

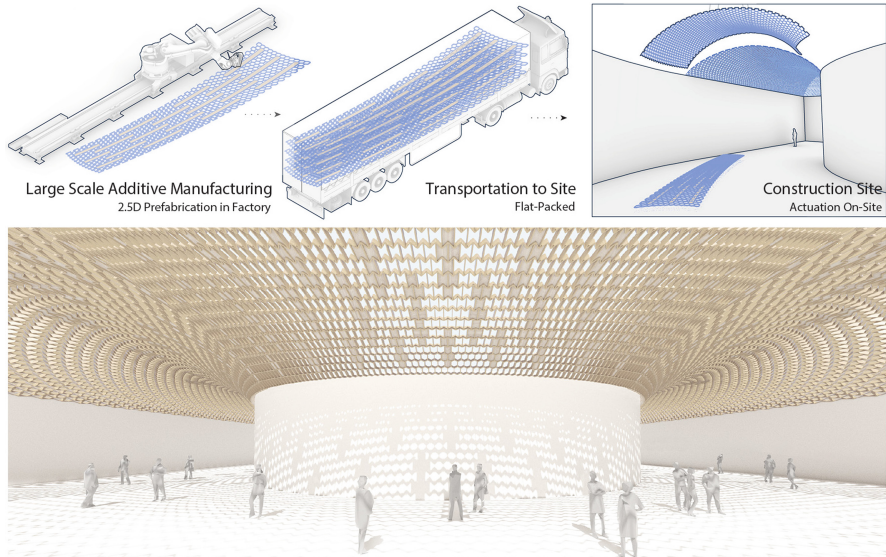


Fig. 8. Concept for the self-shaping of a component based double-curved shell structure

Acknowledgements. This research was conducted as an M.Sc. thesis in the framework of the Integrative Technologies and Architectural Design Research (ITECH) program at the University of Stuttgart, led by the Institute for Computational Design and Construction (ICD), and the Institute of Building Structures and Structural Design (ITKE). The research was supported by the Sino-German Center for Research Promotion: DFG and NSFC through the project Performative Design Methodology based on Robotic Fabrication for Sustainable Architecture (GZ 1162). T. Cheng, S. Leder, D. Wood, A. Menges acknowledge the support of the German Research Foundation under Germany's Excellence Strategy - EXC 2120/1 – 390831618. Printing materials were sponsored by UPM Formi. The authors especially thank Riccardo La Magna for his advice on auxetic metamaterials, Michael Schneider and Michael Preisack for their help in the faculty wood workshop, Urs Basalla and the Institute for Engineering Geodesy for laser scanning, Zied Bhiri, and BEC GmbH and Lucas Janssen of CEAD GB.V. for their extended efforts in robotic extrusion integration.

References

1. Malek, S., Williams, C.J.K.: Reflections on the structure, mathematics and aesthetics of shell structures. *Nexus Netw. J.* **19**(3), 555–563 (2017). <https://doi.org/10.1007/s00004-017-0356-6>. Accessed 5 Mar 2021
2. Rippmann, M., Lachauer, L., Block, P.: Interactive vault design. *Int. J. Space Struct.* **27**(4), 219–230 (2012). <http://journals.sagepub.com/doi/10.1260/0266-3511.27.4.219>. Accessed 10 Mar 2021
3. Groenewolt, A., Schwinn, T., Nguyen, L., Menges, A.: An interactive agent-based framework for materialization-informed architectural design. *Swarm Intell.* **12**(2), 155–186 (2018). <https://doi.org/10.1007/s11721-017-0151-8>. Accessed 15 Mar 2021
4. Wood, D.M., Correa, D., Krieg, O.D., Menges, A.: Material computation-4D timber construction: towards building-scale hygroscopic actuated, self-constructing timber surfaces. *Int. J. Archit. Comput.* **14**(1), 49–62 (2016). <https://doi.org/10.1177/1478077115625522>
5. Tibbits, S. (ed.): *Active Matter*, 351 pp. MIT Press, Cambridge (2017)
6. Boley, J.W., et al.: Shape-shifting structured lattices via multimaterial 4D printing. *Proc. Natl. Acad. Sci.* **116**(42), 20856–20862 (2019). <http://www.pnas.org/lookup/doi/10.1073/pnas.1908806116>. Accessed 12 Mar 2021
7. Aldinger, L., Margariti, G., Körner, A., Suzuki, S., Knippers, J.: Tailoring Self-formation fabrication and simulation of membrane-actuated stiffness gradient composites. In: *Proceedings of the IASS Annual Symposium*. MIT, Boston (2018)
8. Hoadley RB. *Understanding wood: A Craftsman's Guide to Wood Technology*, 280 pp. Taunton Press, Newtown (2000)
9. Menges, A.: *Performative Wood: integral computational design for timber constructions*. In: *Proceeding of the 29th Conference of the Association for Computer Aided Design in Architecture*, Chicago, USA, pp. 66–74 (2009)
10. Wood, D., et al.: From machine control to material programming: self-shaping wood manufacturing of a high performance curved CLT structure - Urbach Tower. In: *Fabricate 2020: Making Resilient Architecture*, pp. 50–57. UCL Press, London (2020). <https://doi.org/10.2307/j.ctv13xpsvw.11>. Accessed 10 Mar 2021
11. Wood, D., Vailati, C., Menges, A., Rüggeberg, M.: Hygroscopically actuated wood elements for weather responsive and self-forming building parts – facilitating upscaling and complex shape changes. *Constr. Build. Mater.* **165**, 782–791 (2018). <https://doi.org/10.1016/j.conbuildmat.2017.12.134>
12. Grönquist, P., Wood, D., Wittel, F.K., Rüggeberg, M.: 4D self-shaping mechanisms for achieving double-curved wooden structures. In: *CompWood 2019: book of abstracts*, p. 25. Växjö, Sweden (2019)
13. Cheng, T., Wood, D., Wang, X., Yuan, P.F.: Programming material intelligence: an additive fabrication strategy for self-shaping biohybrid components. In: Vouloutsis, V., Mura, A., Tauber, F., Speck, T., Prescott, T.J., Verschure, P.F.M.J. (eds.) *Biomimetic and Biohybrid Systems*. *Living Machines 2020*. LNCS, vol. 12413, pp. 36–45. Springer, Cham (2020). https://doi.org/10.1007/978-3-030-64313-3_5
14. Yuan, P.F., Block, P.: *Robotic Force Printing: A Joint Workshop of MIT/ETH/TJ*. Tongji University Press, Shanghai (2019)
15. Naboni, R., Mirante, L.: Metamaterial computation and fabrication of auxetic patterns for architecture, pp. 129–136 (2015). <http://dx.doi.org/10.5151/despro-sigradi2015-30268>

16. Lienhard, J., Gengnagel, C.: Recent developments in bending-active structures. In: Creativity in Structural Design, annual Symposium of the IASS, Boston, USA, p. 11 (2018)
17. Peliński, K., Smardzewski, J., Narojczyk, J.: Stiffness of synclastic wood-based auxetic sandwich panels. *Phys. Status Solidi B* **257**(10), 1900749 (2020). <https://onlinelibrary.wiley.com/doi/10.1002/pssb.201900749>. Accessed 2 Mar 2021
18. La Magna, R.: Bending-active plates: strategies for the induction of curvature through the means of elastic bending of plate-based structures. Doctoral thesis (2017). <https://doi.org/10.18419/opus-9389>
19. Grönquist, P., Wittel, F.K., Rüggeberg, M.: Modeling and design of thin bending wooden bilayers. *PLoS ONE* **13**(10) (2018). <https://doi.org/10.1371/journal.pone.0205607>
20. Sossou, G., Demoly, F., Belkebir, H., Qi, H.J., Gomes, S., Montavon, G.: Design for 4D printing: a voxel-based modeling and simulation of smart materials. *Mater. Des.* **175**, 107798–107798 (2019). <https://doi.org/10.1016/j.matdes.2019.107798>
21. Estrada, R.D., Araujo, A., Guiducci, L., Iglesias, R.M.: Assisting tool for designing hygroscopic systems. M.A. Thesis, Humboldt University, Berlin (2019)
22. Preisinger, C.: Linking structure and parametric geometry. *Archit. Des.* **83**(2), 110–113 (2013). <https://doi.org/10.1002/ad.1564>. Accessed 20 Oct 2020
23. Cheng, T., Tahouni, Y., Wood, D., Stolz, B., Mülhaupt, R., Menges, A.: Multifunctional mesostructures: design and material programming for 4D-printing. In: Symposium on Computational Fabrication. Virtual Event, pp. 1–10. ACM, USA (2020). <https://doi.org/10.1145/3424630.3425418>. Accessed 9 Mar 2021

Open Access This chapter is licensed under the terms of the Creative Commons Attribution 4.0 International License (<http://creativecommons.org/licenses/by/4.0/>), which permits use, sharing, adaptation, distribution and reproduction in any medium or format, as long as you give appropriate credit to the original author(s) and the source, provide a link to the Creative Commons license and indicate if changes were made.

The images or other third party material in this chapter are included in the chapter's Creative Commons license, unless indicated otherwise in a credit line to the material. If material is not included in the chapter's Creative Commons license and your intended use is not permitted by statutory regulation or exceeds the permitted use, you will need to obtain permission directly from the copyright holder.

